JACS
JOURNAL OF THE AMERICAN CHEMICAL SOCIETY

Article

pubs.acs.org/JACS

Mechanism Studies of Ir-Catalyzed Asymmetric Hydrogenation of Unsaturated Carboxylic Acids

Mao-Lin Li,[†,§] Shuang Yang,[†,§] Xun-Cheng Su,[†] Hui-Ling Wu,[†] Liang-Liang Yang,[†] Shou-Fei Zhu,*[,†] and Qi-Lin Zhou*[,†,‡]

[†]State Key Laboratory and Institute of Elemento-Organic Chemistry, Nankai University, Tianjin 300071, China

[‡]Collaborative Innovation Center of Chemical Science and Engineering (Tianjin), Nankai University, Tianjin 300071, China

Supporting Information

ABSTRACT: The Ir-catalyzed asymmetric hydrogenation of olefins is widely used for production of value-added bulk and fine chemicals. The iridium catalysts with chiral spiro phosphine-oxazoline ligands developed in our group show high activity and high enantioselectivity in the hydrogenation of olefins bearing a coordinative carboxyl group, such as α,β-unsaturated carboxylic acids, β,γ-unsaturated carboxylic acids, and γ,δ-unsaturated carboxylic acids. Here we conducted detailed mechanistic studies on these Ir-catalyzed asymmetric hydrogenation reactions by using (*E*)-2-methyl-3-phenylacrylic acid as a model substrate. We isolated and characterized several key intermediates having Ir−H bonds under the real hydrogenation conditions. Particularly, an Ir(III) migratory insertion intermediate was first isolated in an asymmetric hydrogenation reaction promoted by chiral Ir catalysts. That this intermediate cannot undergo reductive elimination in the absence of hydrogen strongly supports the involvement of an Ir(III)/Ir(V) cycle in the hydrogenation. On the basis of the structure of the Ir(III) intermediate, variable-temperature NMR spectroscopy, and density functional theory calculations, we elucidated the mechanistic details of the Ir-catalyzed hydrogenation of unsaturated carboxylic acids and explained the enantioselectivity of the reactions. These findings experimentally and computationally elucidate the mechanism of Ir-catalyzed asymmetric hydrogenation of olefins with a strong coordinative carboxyl group and will likely inspire further catalyst design.

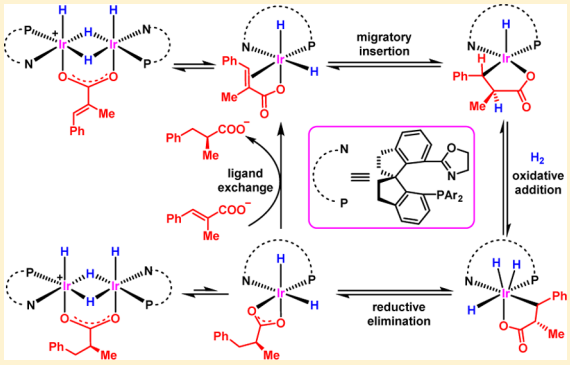

INTRODUCTION

Owing to its perfect atom economy, operational simplicity, and mild reaction conditions, transition-metal-catalyzed asymmetric hydrogenation of unsaturated compounds is becoming a very important method for the production of chiral value-added bulk and fine chemicals. Studies of the mechanism have attracted considerable interest[1] because mechanistic information and the isolation of key active intermediates can guide the rational design of new chiral catalysts. The Rh complexes of chiral diphosphine ligands (chiral analogues of Wilkinson catalyst) and Ir complexes of chiral P,N-ligands (chiral analogues of Crabtree catalyst) are the most representative chiral catalysts for the asymmetric hydrogenation of olefins.[1] Generally speaking, Rh- or Ir-catalyzed asymmetric hydrogenation of olefins involves activation of both hydrogen and a substrate, and the catalytic cycle consists of three basic steps: oxidative addition of hydrogen to the transition metal atom M (Rh or Ir), migratory insertion of the unsaturated group of the substrate into the M−H bond, and reductive elimination of the metal from the migratory insertion intermediate (Figure 1). Migratory insertion intermediates **I** are particularly valuable for mechanistic studies because they contain both of the activated reaction components (hydrogen and the olefin substrate) and can therefore provide the evidence for understanding chiral induction by the catalyst. Benefiting from the characterization of migratory insertion intermediates of chiral Rh-diphosphine catalysts through NMR at low temperature, the catalytic cycle of Rh-catalyzed asymmetric hydrogenation of olefins has been well-established.[2]

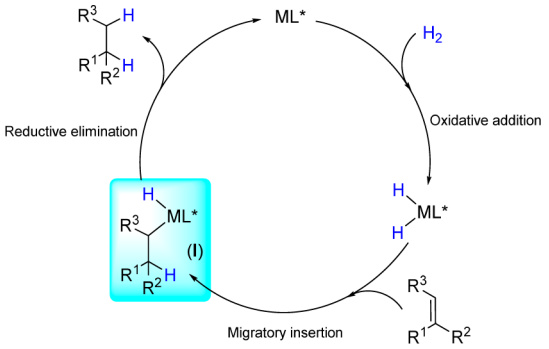

Figure 1. Schematic of the catalytic cycles for transition-metal-catalyzed asymmetric hydrogenation reactions. M = Rh or Ir; L* = chiral ligand.

Received: November 16, 2016
Published: December 12, 2016

DOI: 10.1021/jacs.6b11655
J. Am. Chem. Soc. 2017, 139, 541−547

However, although extensive mechanistic studies of Ir-catalyzed asymmetric hydrogenation of unfunctionalized olefins have been conducted through isolation of active intermediates or calculations,[3] the migratory insertion intermediates of chiral Ir catalysts have, to the best of our knowledge, never been isolated and characterized.[4] As a result, the mechanism of Ir-catalyzed asymmetric hydrogenation still lacks a critical jigsaw. Because of containing highly active M−H bond and M−C bond, the migratory insertion intermediates of the Ir-catalyzed hydrogenation of olefins are very unstable and difficult to isolate and characterize.

We recently developed iridium catalysts with chiral spiro phosphine-oxazoline (SIPHOX) ligands (Figure 2).[5] Unlike the

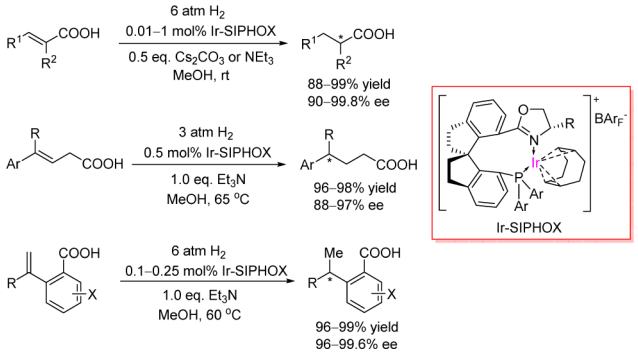

Figure 2. Ir-SIPHOX-catalyzed enantioselective hydrogenation of olefins containing a coordinative carboxy group.

other chiral iridium catalysts with phosphine-oxazoline ligands, which exhibit high activity as well as enantioselectivity in the hydrogenation of unfunctionalized olefins, the Ir-SIPHOX catalysts showed excellent activity and enantioselectivity in the hydrogenation of olefins bearing a coordinative carboxyl group, such as α,β-unsaturated carboxylic acids,[6] β,γ-unsaturated carboxylic acids,[7] and γ,δ-unsaturated carboxylic acids.[8] The high stability of these catalysts under hydrogenation conditions[5] allows us to probe the mechanism of the Ir-catalyzed asymmetric hydrogenation by trapping the active intermediates. Herein we report our findings in the study of the mechanism of asymmetric hydrogenations catalyzed by Ir-SIPHOX catalysts: specifically, we describe the first isolation and identification of an active Ir(III) migratory insertion intermediate. That the Ir(III) migratory insertion intermediate cannot undergo reductive elimination in the absence of hydrogen gas provides strong evidence to support the involvement of an Ir(III)/Ir(V) cycle in these reactions. On the basis of the reactivity of the Ir(III) migratory insertion intermediate, variable-temperature nuclear magnetic resonance (NMR) spectroscopy experiments, and density functional theory (DFT) calculations, we explain the enantioselectivity of these reactions. Our findings elucidate the mechanism of Ir-catalyzed asymmetric hydrogenation of olefins with strong coordinative groups.

RESULTS AND DISCUSSION

Isolation of Iridium Migratory Insertion Intermediate.

Treatment of chiral Ir-SIPHOX catalyst (S_a)-**1**[9] with hydrogen gas in methanol solution at 25 °C produced an Ir-dihydride species in quantitative yield (Figure 3). NMR spectroscopy and high-resolution mass spectrometry clearly indicated that this species was either **2a** or **2b**. This assignment was based on the observation of the ^{1}H NMR signal for P−Ir−H as a double

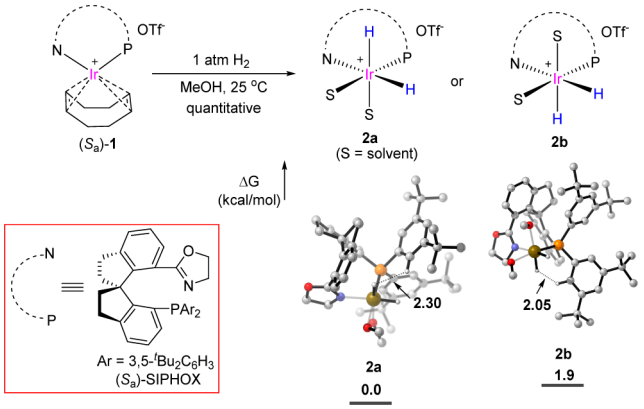

Figure 3. Preparation of an iridium dihydride species.

doublet at −20.23 and −31.01 ppm (ppm) (J_{P-H} = 20.8 and 24.8 Hz, where J is the coupling constant between the phosphorus and the hydride) and the ^{31}P NMR signal as a singlet at 22.82 ppm (see Supporting Information, SI, Figures S1 and S5). This result indicated that the oxidative addition of the H−H bond to the Ir atom generated an iridium dihydride in which the two hydrides are oriented *cis* to the phosphorus atom of the ligand because the strong *trans* effect of the phosphorus atom weakened the *trans* Ir−H bond.[10] DFT calculations showed that the distances between the axial hydride and one of the hydrogen atoms on the phenyl ring of the ligand differ in the two Ir-dihydride species (2.30 and 2.05 Å in **2a** and **2b**, respectively) and that **2a** is more stable than **2b**.[11] The calculations also suggested that **2a** and **2b** may be in kinetic equilibrium during the hydrogenation. However, because **2a** is the more thermodynamically stable product and because its calculated structure is more consistent with the NMR results, we suggest that **2a** is the most likely product.

Treatment of **2a** with 1 equiv of sodium (*E*)-2-methyl-3-phenyl acrylate in methanol at 25 °C generated migratory insertion product **3** in 97% yield within 5 min (Figure 4, eq a). All of the organic components of **3**, including the SIPHOX ligand and the partially hydrogenated substrate, were unambiguously identified by means of NMR spectroscopy. We assigned the coordination geometry of this chiral octahedral iridium complex on the basis of ligand field theory. The observation of a doublet at −31.51 ppm (see SI, Figure S12, $^2J_{P-H}$ = 29.2 Hz) in the ^{1}H NMR spectrum indicated that the hydride was opposite to a vacant orbital or to a coordinated solvent molecule (MeOH); this determination was made on the basis of previously reported data for Ir-hydride complexes.[3n,12] The ^{1}H NMR spectrum also showed a doublet ($^3J_{H-H}$ = 6.8 Hz) for the methyl group of the partially hydrogenated substrate, confirming that a hydride in **2a** had been transferred to the α-carbon of the carboxyl group in the substrate. In the ^{13}C NMR (see SI, Figures S14 and S15) and two-dimensional NMR spectra of **3** (see SI, Figures S16−S20), the coupling constants between the phosphorus and the Ir−C (δ = 17.8 ppm, $^2J_{P-C}$ = 76 Hz) and between the phosphorus and the α-carbon of the carboxyl group (δ = 49.5 ppm, $^3J_{P-C}$ = 10 Hz) implied that the Ir−C was located *trans* to the phosphorus atom. Nuclear Overhauser effect spectroscopy clearly showed interactions between the hydrogen on the benzene ring of the substrate and the hydrogen on the oxazoline ring of the ligand, and these results also supported the *trans* location of the Ir−C relative to the phosphorus atom. Additionally, the exact formula

DOI: 10.1021/jacs.6b11655
J. Am. Chem. Soc. 2017, 139, 541−547

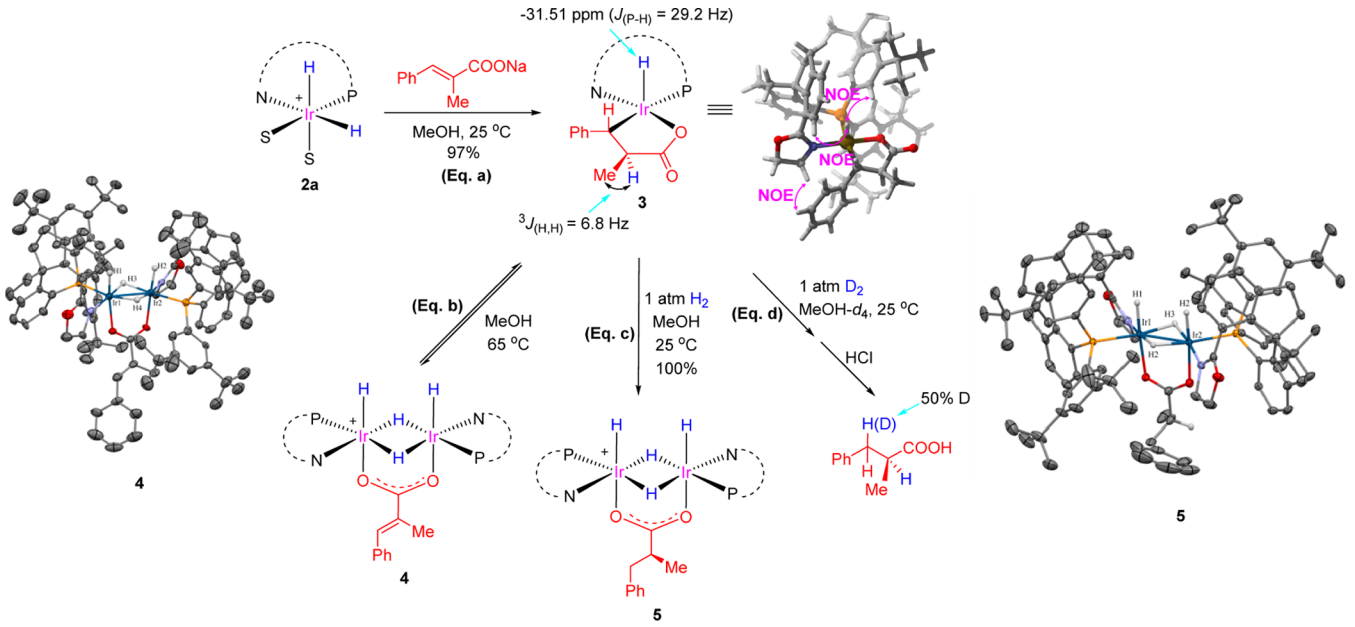

Figure 4. Structural analysis and transformations of migratory insertion intermediate **3**.

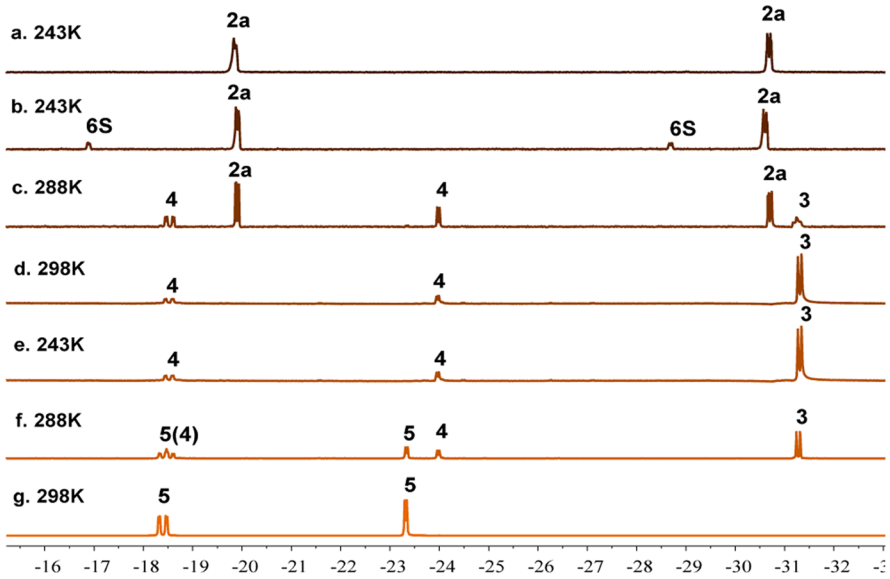

Figure 5. Variable-temperature ^{1}H NMR analysis of the hydrogenation in CD_3OD.

of **3** was confirmed by high-resolution mass spectrometry (calcd for $C_{58}H_{72}IrNO_3P^+$, 1054.4874; found, 1054.4860). Hence, the three-dimensional structure of **3** was assigned as shown in Figure 4. The carboxyl group of **3** played an important role in stabilizing the structure, which enabled us to isolate this Ir(III) migratory insertion intermediate.

Intermediate **3** cannot undergo reductive elimination spontaneously in the absence of hydrogen gas. However, when **3** was heated or kept in solution for 24 h, it underwent β-H elimination and subsequent formation of binuclear complex **4**, which has only one unsaturated carboxylate (Figure 4, eq b). However, our attempts to grow a single crystal of **3** resulted in the formation of a single crystal of **4** instead. X-ray diffraction analysis of **4** showed that the carboxyl group bridges two iridium centers, each of which has an axial terminal hydride (H1 and H2, crystal **4**, Figure 4).[13] Note that a triflate anion has been omitted from all the structures for clarity.

In contrast, under 1 atm of hydrogen, **3** reacted smoothly at 25 °C to form complex **5** within 0.5 h (Figure 4, eq c). X-ray diffraction analysis of a crystal of **5** (the ligands in **5** have *R* configurations) indicated that it, like **4**, has a binuclear structure, but with a fully hydrogenated carboxylate as the bridging ligand. Both **4** and **5** can be used as catalyst precursor for the hydrogenation of (*E*)-2-methyl-3-phenylacrylic acid. Under 1 atm of deuterium, intermediate **3** was hydrogenated to a product containing 50% D at the newly formed C−H(D) bond at the β-position (see SI, Figures S39−S40), which implies that the H atoms involved in the reductive elimination step came from both the hydride of **3** and the hydrogen molecule (see the Discussion below). Clearly, the addition of hydrogen gas was necessary to convert migratory insertion intermediate **3** to the corresponding alkane, and an Ir(V) species might be involved in this process. This experimental result rules out the involvement of an Ir(I)/Ir(III) cycle and

DOI: 10.1021/jacs.6b11655
J. Am. Chem. Soc. 2017, 139, 541−547

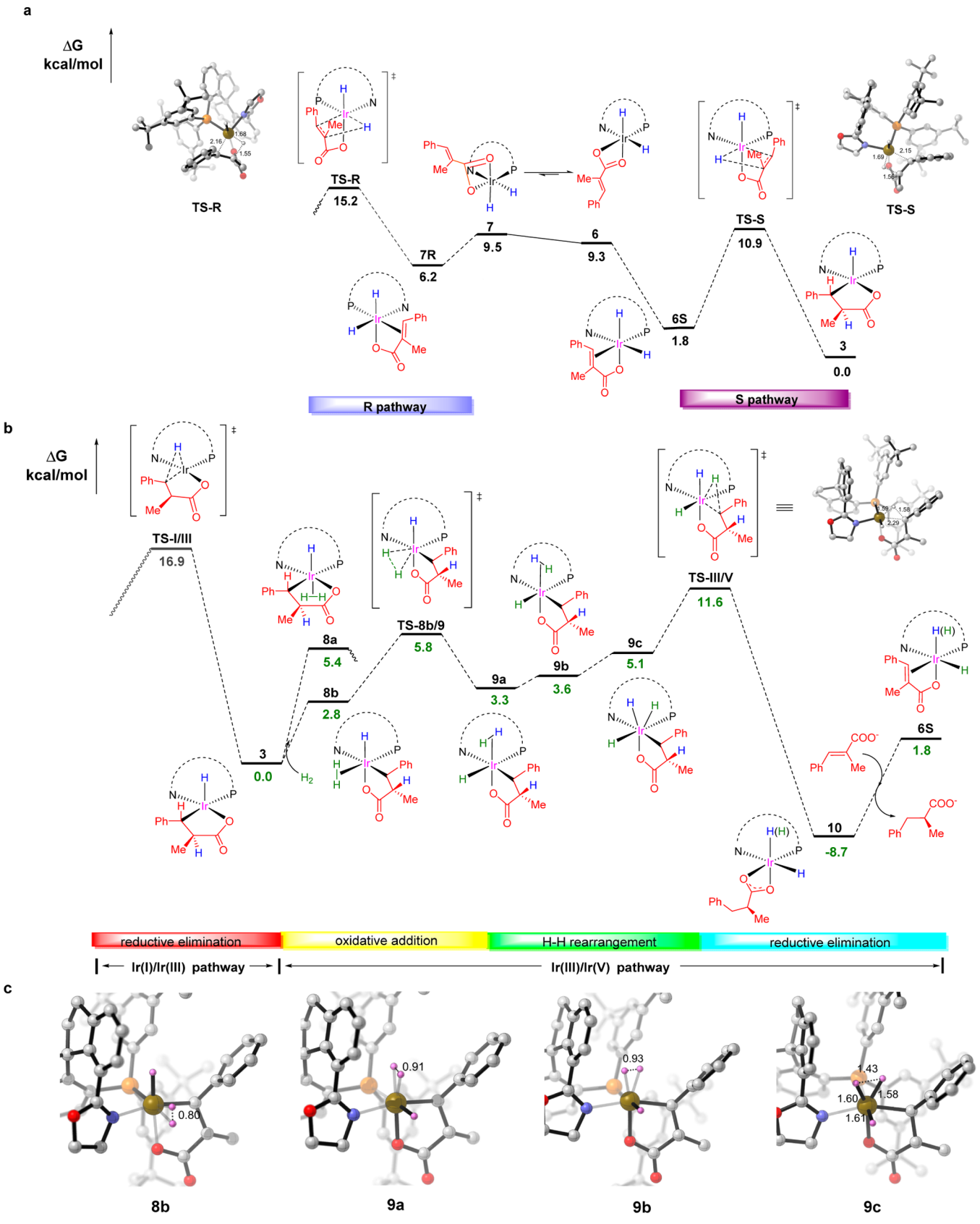

Figure 6. Results of DFT calculations for a model reaction. (a) Calculated Gibbs energy profile for the chiral induction step. The migratory insertion reactions of the two Ir(III) dihydride olefin complexes (**6S** and **7R**) proceed via different four-membered-ring transition states, **TS-R** and **TS-S**, respectively, leading to different products. (b) Calculated Gibbs energy profile for the Ir(III)/Ir(V) and Ir(I)/Ir(III) pathways. The Ir(III)/Ir(V) pathway requires additional H_2 for the oxidative addition reaction of **3** to form **9c**. The calculated energies for reductive elimination reactions via transition states **TS-III/V** and **TS-I/III** are also shown. (c) Oxidative addition of and rearrangement of the H−H bond in going from **8b** to **9c** along the Ir(III)/Ir(V) pathway. Hydrogen atoms bound to carbon are omitted for clarity.

DOI: 10.1021/jacs.6b11655
J. Am. Chem. Soc. 2017, 139, 541−547

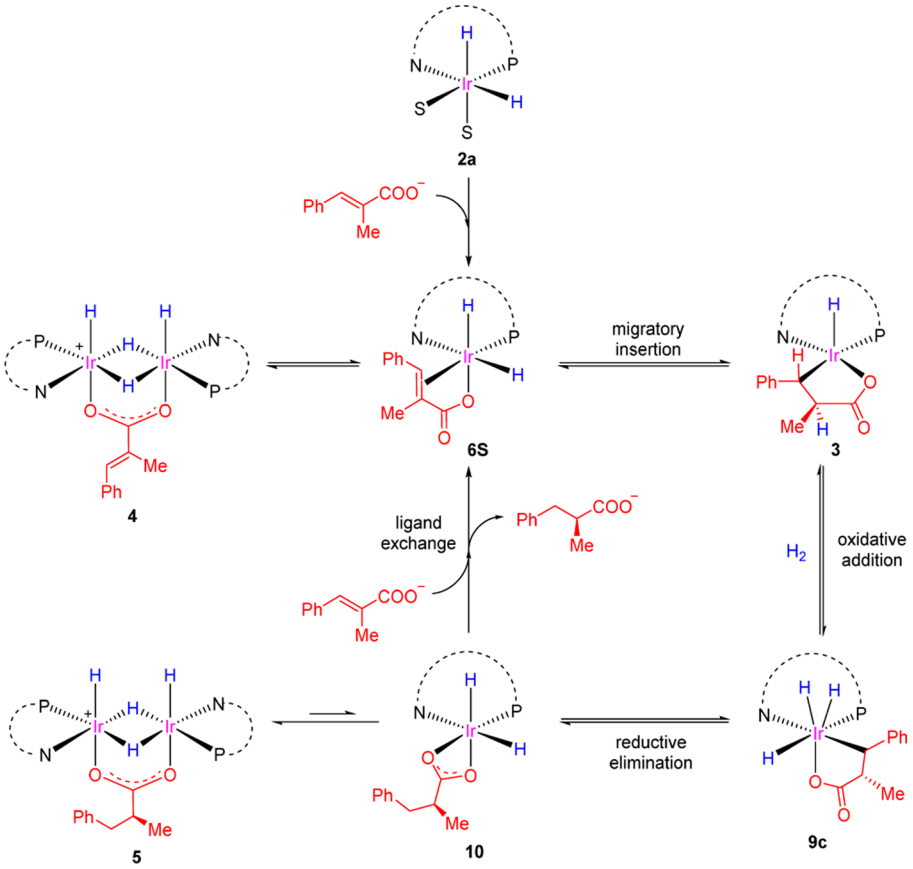

Figure 7. Catalytic cycle for the hydrogenation reaction.

strongly supports an Ir(III)/Ir(V) cycle for the hydrogenation of olefins under these conditions.

Variable-Temperature NMR Experiments. With these key intermediates in hand, we conducted variable-temperature ^{1}H and ^{31}P NMR experiments (see SI, Figure S42) to track the progress of the hydrogenation reaction (Figure 5). When a solution of **2a** in CD_3OD under argon in an NMR tube was treated with sodium (*E*)-2-methyl-3-phenyl acrylate at 243 K, a set of new iridium hydride signals appeared (Figure 5b). By analogy to Pfaltz's observations,[3n] we attributed these new signals to Ir(III) dihydride olefin complex **6S** (see its structure in Figures 6 and 7), an intermediate that formed prior to migratory insertion. At 288 K, the signals of **6S** disappeared, and signals of **3** and **4** appeared (Figure 5c). When the temperature was increased to 298 K and kept there for 10 min, most of the **4** was transformed to migratory insertion intermediate **3** (containing about 5% of **4**) (Figure 5d). The solution of **3** was then treated with hydrogen gas as the temperature was increased from 243 to 298 K (Figure 5e–g). The transformation of **3** to **5** started at 288 K and was complete by the time the temperature reached 298 K.

Computational Studies. To improve our understanding of the details of the reaction mechanism, we performed DFT studies using the reaction of iridium dihydride **2a** with (*E*)-2-methyl-3-phenylacrylic acid as a model. First, we calculated the chiral induction step, conversion of **2a** to **3** (Figure 6a).[14] There are two possible pathways for the formation of migratory insertion product **3** from **2a**, which are designated the *R* pathway and the *S* pathway (Figure 6a) and which proceed via different olefin coordination models (**6S** and **7R**, respectively) with the equilibration between **6** and **7**.[15] The calculated energy of transition state **TS-S** was 4.3 kcal/mol lower than that of transition state **TS-R**, which suggests that the reaction should proceed with perfect enantioselectivity to afford the *S* product, which is consistent with the experimental result (99% ee, with *S* configuration).

Numerous attempts to isolate an Ir(V) intermediate were unsuccessful. We attribute this to the high thermal instability of such intermediates. Fortunately, DFT studies can provide insight into the formation and reactions of Ir(V) intermediates (Figure 6b,c). According to our calculations, coordination of a hydrogen molecule to Ir(III) complex **3** can give either of the two isomeric Ir(III) dihydrogen complexes, **8a** or **8b**. Our calculations suggest that **8b**, which is more stable than **8a**, has a lower energy barrier in the subsequent oxidative addition transition state **TS-8b/9**. Interestingly, **8b** cannot directly form Ir(V) trihydride intermediate **9c** via **TS-8b/9**; instead, **8b** rearranges to **9a** and then **9b**, which in turn undergoes oxidative addition to afford **9c**. This high-valent structure readily undergoes reductive elimination via transition state **TS-III/V** with an 11.6 kcal/mol energy barrier, which is 5.3 kcal/mol lower than that for transition state **TS-I/III**. Like the experimental results, the DFT results suggest that the hydrogenation reaction preferentially proceeds via an Ir(III)/Ir(V) pathway. The unexpected hydrogen rearrangement sequence from **8b** to **9c** (Figure 6b) explains the deuterium distribution in the product of the deuteration experiment (Figure 4, eq d). In the reductive elimination of **9c**, only the hydrogen or the deuterium in the N–O–C–Ir plane can participate in the reaction. Because the N–O–C–Ir plane in **9c** contains one hydrogen and one deuterium, the reductive elimination reaction gives a product containing 50% D at the

DOI: 10.1021/jacs.6b11655
J. Am. Chem. Soc. 2017, 139, 541–547

newly formed C−H bond at the β-position. Another two alternative mechanisms to generate Ir(V) including a concerted oxidative addition of side-on bound H_2 with concomitant reductive elimination mechanism (see SI, Figures S45−S46) were also calculated, but both exhibit an unfavorable energy barrier in comparison with the pathway of Figure 6b.

Ir(III)/Ir(V) Catalytic Cycle. Taken together, our results suggest that the hydrogenation reaction proceeds via the catalytic cycle shown in Figure 7. The cycle starts with iridium dihydride complex **6S**, which was formed from a coordination of unsaturated carboxylate substrate to the iridium dihydride **2a**, which in turn undergoes migratory insertion of an Ir−H bond to give intermediate **3**. In addition, bridging of two molecules of Ir(III) species **2a** with a single unsaturated carboxylate molecule can result in the formation of dimer **4**. Intermediate **3** is further oxidized by hydrogen to Ir(V) species **9c**, which undergoes a reductive elimination to give an intermediate **10**. The ligand exchange of intermediate **10** with unsaturated carboxylate substrate releases the hydrogenation product and regenerates the iridium dihydride complex **6S**. The carboxyl group of the hydrogenation product, saturated carboxylate, can also serve as a bridging ligand to generate dimer **5**, which serves as a resting catalyst for the next cycle. Intermediates **2a**, **3**, **4**, **5**, and **6S** were unequivocally identified experimentally. The structures of Ir(V) intermediate **9c** and Ir(III) intermediate **10**, chiral induction transition state **TS-S**, and transition state **TS-III/V** were obtained by means of DFT calculations.

It is noteworthy that an Ir-dihydride-olefin complex identified as an intermediate in the hydrogenation of an unfunctionalized substrate[3n] does not undergo migratory insertion in the absence of H_2, in contrast to the findings in this study. In another study using a lactone with an exocyclic C=C bond as substrate,[3o] evidence for an Ir(I)/(III) mechanism was found. This mechanistic divergence indicates that the mechanism of Ir-catalyzed hydrogenation of alkenes may vary depending on the type of substrate and/or catalyst.

CONCLUSION

In summary, detailed mechanistic studies on the enantioselective hydrogenation of an unsaturated carboxylic acid catalyzed by an iridium complex with a chiral SIPHOX ligand were conducted. The high stability of the Ir-SIPHOX catalyst enabled us to isolate and fully characterize key intermediates in the hydrogenation process, including intermediate **3**. To our knowledge, this is the first report of the isolation of a migratory insertion intermediate in an asymmetric hydrogenation reaction promoted by chiral Crabtree-type catalysts. That **3** could not undergo reductive elimination in the absence of hydrogen but smoothly gave the hydrogenation product in the presence of hydrogen rules out the Ir(I)/Ir(III) cycle and strongly supports an Ir(III)/Ir(V) cycle. With this information about the intermediates, we tracked the hydrogenation process by means of variable-temperature NMR, and we performed DFT calculations to illustrate the full catalytic cycle and rationalize the enantioselectivity of the reaction. The migratory insertion intermediate contains both of the activated components of the reaction (the hydrogen and the unsaturated substrate) and is the key for studying the reaction pathway and chiral induction by the catalyst. The isolation and characterization of **3** elucidated the mechanism of Ir-catalyzed asymmetric hydrogenation of olefins with a coordinative carboxyl group and will likely inspire further catalyst design.

ASSOCIATED CONTENT

Supporting Information

The Supporting Information is available free of charge on the ACS Publications website at DOI: 10.1021/jacs.6b11655.

Experimental procedures and spectral data (PDF)
Crystallographic data for compound **4** (CIF)
Crystallographic data for compound **5** (CIF)

AUTHOR INFORMATION

Corresponding Authors

*sfzhu@nankai.edu.cn
*qlzhou@nankai.edu.cn

ORCID

Qi-Lin Zhou: 0000-0002-4700-3765

Author Contributions

§M.-L.L. and S.Y. contributed equally.

Notes

The authors declare no competing financial interest.
Metrical parameters for the structures are available free of charge from the Cambridge Crystallographic Data Centre under reference numbers CCDC-1496895 and 1496894.

ACKNOWLEDGMENTS

We thank Dr. Xiao-Song Xue for his constructive discussions on DFT calculations. We thank the National Natural Science Foundation of China, the National Basic Research Program of China (2012CB821600), the "111" project (B06005) of the Ministry of Education of China, and the National Program for Support of Top-Notch Young Professionals for financial support.

REFERENCES

(1) (a) *The Handbook of Homogeneous Hydrogenation*; de Vries, J. G., Elsevier, C. J., Eds.; Wiley-VCH: Weinheim, 2007. (b) Osborn, J. A.; Jardine, F. H.; Young, J. F.; Wilkinson, G. *J. Chem. Soc. A* **1966**, 1711. (c) Crabtree, R. *Acc. Chem. Res.* **1979**, *12*, 331.

(2) (a) Halpern, J. *Science* **1982**, *217*, 401. (b) Brown, J. M. *Organometallics* **2014**, *33*, 5912.

(3) For reviews, see: (a) Cui, X.; Burgess, K. *Chem. Rev.* **2005**, *105*, 3272. (b) Roseblade, S. J.; Pfaltz, A. *Acc. Chem. Res.* **2007**, *40*, 1402. (c) Verendel, J. J.; Pàmies, O.; Diéguez, M.; Andersson, P. G. *Chem. Rev.* **2014**, *114*, 2130. (d) Sperger, T.; Sanhueza, I. A.; Kalvet, I.; Schoenebeck, F. *Chem. Rev.* **2015**, *115*, 9532. For examples, see: (e) Crabtree, R. H.; Demou, P. C.; Eden, D.; Mihelcic, J. M.; Parnell, C. A.; Quirk, J. M.; Morris, G. E. *J. Am. Chem. Soc.* **1982**, *104*, 6994. (f) Brandt, P.; Hedberg, C.; Andersson, P. G. *Chem. - Eur. J.* **2003**, *9*, 339. (g) Dietiker, R.; Chen, P. *Angew. Chem., Int. Ed.* **2004**, *43*, 5513. (h) Fan, Y.; Cui, X.; Burgess, K.; Hall, M. B. *J. Am. Chem. Soc.* **2004**, *126*, 16688. (i) Cui, X.; Fan, Y.; Hall, M. B.; Burgess, K. *Chem. - Eur. J.* **2005**, *11*, 6859. (j) Church, T. L.; Rasmussen, T.; Andersson, P. G. *Organometallics* **2010**, *29*, 6769. (k) Hopmann, K. H.; Bayer, A. *Organometallics* **2011**, *30*, 2483. (l) Mazuela, J.; Norrby, P. O.; Andersson, P. G.; Pàmies, O.; Diéguez, M. *J. Am. Chem. Soc.* **2011**, *133*, 13634. (m) Sparta, M.; Riplinger, C.; Neese, F. *J. Chem. Theory Comput.* **2014**, *10*, 1099. (n) Gruber, S.; Pfaltz, A. *Angew. Chem., Int. Ed.* **2014**, *53*, 1896. (o) Liu, Y.; Gridnev, I. D.; Zhang, W.-B. *Angew. Chem., Int. Ed.* **2014**, *53*, 1901. (p) Polo, V.; Al-Saadi, A. A.; Oro, L. A. *Organometallics* **2014**, *33*, 5156. (q) Hopmann, K. H.; Frediani, L.; Bayer, A. *Organometallics* **2014**, *33*, 2790. (r) Borrãs, C.; Biosca, M.; Pãmies; Diéguez, M. *Organometallics* **2015**, *34*, 5321. (s) Engel, J.; Mersmann, S.; Norrby, P.; Bolm, C. *ChemCatChem* **2016**, *8*, 3099.

(4) An alkyl Ir hydride complex with a chiral P,N ligand was isolated by Maurer and Kazmaier; however, it was proven to be an inactive component towards the hydrogenation. (a) Maurer, F.; Kazmaier, U. *J.*

DOI: 10.1021/jacs.6b11655
J. Am. Chem. Soc. 2017, 139, 541−547

Org. Chem. **2013**, *78*, 3425. A migratory insertion intermediate of Ru catalyst has been isolated and characterized in an asymmetric hydrogenation reaction. However, the mechanism is different; it contains a heterolytic H_2 activation. (b) Wiles, J. A.; Bergens, S. H.; Young, V. G. *J. Am. Chem. Soc.* **1997**, *119*, 2940.
(5) Zhu, S.-F.; Xie, J.-B.; Zhang, Y.-Z.; Li, S.; Zhou, Q.-L. *J. Am. Chem. Soc.* **2006**, *128*, 12886.
(6) (a) Li, S.; Zhu, S.-F.; Zhang, C.-M.; Song, S.; Zhou, Q.-L. *J. Am. Chem. Soc.* **2008**, *130*, 8584. (b) Li, S.; Zhu, S.-F.; Xie, J.-H.; Song, S.; Zhang, C.-M.; Zhou, Q.-L. *J. Am. Chem. Soc.* **2010**, *132*, 1172. (c) Song, S.; Zhu, S.-F.; Pu, L.-Y.; Zhou, Q.-L. *Angew. Chem., Int. Ed.* **2013**, *52*, 6072. (d) Song, S.; Zhu, S.-F.; Li, Y.; Zhou, Q.-L. *Org. Lett.* **2013**, *15*, 3722.
(7) Song, S.; Zhu, S.-F.; Yang, S.; Li, S.; Zhou, Q.-L. *Angew. Chem., Int. Ed.* **2012**, *51*, 2708.
(8) (a) Song, S.; Zhu, S.-F.; Yu, Y.-B.; Zhou, Q.-L. *Angew. Chem., Int. Ed.* **2013**, *52*, 1556. (b) Yang, S.; Zhu, S.-F.; Guo, N.; Song, S.; Zhou, Q.-L. *Org. Biomol. Chem.* **2014**, *12*, 2049.
(9) The catalysts with $BArF^-$ or OTf^- as the anion gave the same results (99% yield and 99% ee) in the hydrogenation of (*E*)-2-methyl-3-phenylacrylic acid. For simplifying the NMR analysis, we used (S_a)-**1** in our study.
(10) (a) Mazet, C.; Smidt, S. P.; Meuwly, M.; Pfaltz, A. *J. Am. Chem. Soc.* **2004**, *126*, 14176. (b) Crabtree, R. H. *The Organometallic Chemistry of the Transition Metals*, 6th ed.; Wiley, 2014.
(11) (a) Bondi, A. *J. Phys. Chem.* **1964**, *68*, 441. (b) Rowland, R. S.; Taylor, R. *J. Phys. Chem.* **1996**, *100*, 7384.
(12) (a) Scott, N. M.; Pons, V.; Stevens, E. D.; Heinekey, D. M.; Nolan, S. P. *Angew. Chem., Int. Ed.* **2005**, *44*, 2512. (b) Castillo, M. R.; Martín, M.; Fraile, J. M.; Mayoral, J. A.; Sola, E. *Angew. Chem., Int. Ed.* **2011**, *50*, 3240.
(13) For other dinuclear iridium hydride complexes, see: Gruber, S.; Neuburger, M.; Pfaltz, A. *Organometallics* **2013**, *32*, 4702.
(14) Different isomeric transition states have been calculated (see SI, Figure S44), and the one with lowest energy is presented in Figure 6.
(15) For a similar equilibration, see: Gruber, S. *Organometallics* **2016**, *35*, 699.

DOI: 10.1021/jacs.6b11655
J. Am. Chem. Soc. 2017, 139, 541−547